





Article

Paleohistological inferences of thermometabolic regimes in Notosuchia (Pseudosuchia: Crocodylomorpha) revisited

Jorge Cubo* , Paul Aubier , Mathieu G. Faure-Brac , Gaspard Martet, Romain Pellarin, Idriss Pelletan, and Mariana V. A. Sena 

Abstract.—Notosuchia is a group of mostly terrestrial crocodyliforms. The presence of a prominent crest overhanging the acetabulum, slender straight-shafted long bones with muscular insertions close to the joints, and a stable knee joint suggests that they had an erect posture. This stance has been proposed to be linked to endothermy, because it is present in mammals and birds and contributes to the efficiency of their respiratory systems. However, a bone paleohistological study unexpectedly suggested that Notosuchia were ectothermic organisms. The thermophysiological status of Notosuchia deserves further analysis, because the methodology of the previous study can be improved. First, it was based on a relationship between red blood cell size and bone vascular canal diameter tested using 14 extant tetrapod species. Here we present evidence for this relationship using a more comprehensive sample of extant tetrapods (31 species). Moreover, contrary to previous results, bone cross-sectional area appears to be a significant explanatory variable (in addition to vascular canal diameter). Second, red blood cell size estimations were performed using phylogenetic eigenvector maps, and this method excludes a fraction of the phylogenetic information. This is because it generates a high number of eigenvectors requiring a selection procedure to compile a subset of them to avoid model overfitting. Here we inferred the thermophysiology of Notosuchia using phylogenetic logistic regressions, a method that overcomes this problem by including all of the phylogenetic information and a sample of 46 tetrapods. These analyses suggest that *Araripesuchus wegeneri*, *Armadillosuchus arrudai*, *Baurusuchus* sp., *Iberosuchus macronodon*, and *Stratiosuchus maxhechti* were ectothermic organisms.

Jorge Cubo, Paul Aubier, Mathieu G. Faure-Brac, Gaspard Martet, Romain Pellarin, and Idriss Pelletan. Sorbonne Université, Muséum national d'Histoire naturelle, CNRS, Centre de Recherche en Paléontologie—Paris (CR2P, UMR 7207), Paris, France. E-mail: jorge.cubo_garcia@sorbonne-universite.fr, paul.aubier@gmail.com, faurebrac.mathieu@gmail.com, gaspard.martet@gmail.com, romain.pellarin74@gmail.com, idriss.pelletan@laposte.net

Mariana V. A. Sena. Sorbonne Université, Muséum national d'Histoire naturelle, CNRS, Centre de Recherche en Paléontologie—Paris (CR2P, UMR 7207), Paris, France; and Laboratório de Paleontologia da URCA-LPU, Centro de Ciências Biológicas e da Saúde, Universidade Regional do Cariri, Rua Carolino Sucupira-Pimenta, Crato, Ceará 63105-010, Brazil. E-mail: mari.araujo.sena@gmail.com

Accepted: 14 July 2022

*Corresponding author.

Introduction

Notosuchia is a group of extinct, mostly terrestrial crocodyliforms. The presence of several morphological features suggests that they had an erect posture: the prominent crest overhanging the acetabulum observed in *Chimaerasuchus paradoxus* (Wu and Sues 1996), *Notosuchus terrestris* (Pol 2005), *Araripesuchus tsangatsangana* (Turner 2006), *Baurusuchus albertoi* (Nascimento and Zaher 2010), and *Stratiosuchus maxhechti* (Riff and Kellner 2011); the straight-shafted long bones described in

Anatosuchus minor and *Araripesuchus* spp. (Serenó and Larsson 2009); the slender limb bones with muscular insertions close to the joints reported in *Malawisuchus mwakasyungutiensis* (Gomani 1997); and the tight/stable knee joint shown in *Pissarrachampsia sera* (Godoy et al. 2016). Among extant tetrapods, only endotherms (mammals and birds) show an upright stance. This last feature has been proposed to be linked to endothermy, because it contributes to the efficiency of the respiratory system (Carrier 1987). Thus, according to this morphological evidence,

we can reasonably hypothesize that Notosuchia were endothermic. However, Cubo et al. (2020) concluded that they were primitively ectothermic using two proxies: resting metabolic rate (RMR) and red blood cell size (RBC_{size}).

RMR is the minimal consumption of oxygen over time per unit of body mass measured under postabsorptive conditions during the period of normal activity of the daily cycle in resting, nonreproductive specimens (Andrews and Pough 1985; Montes et al. 2007). RMRs of extant endotherms are at least one order of magnitude higher than those of extant ectotherms of similar body mass, because the mechanisms of thermogenesis operating in the former are costly in terms of energy (Clarke and Pörtner 2010; Legendre and Davesne 2020). RMRs inferred by Cubo et al. (2020) for Notosuchia were significantly lower than the threshold separating ectotherms from endotherms.

Within extant tetrapods, RBC_{size} is lower in endotherms (mammals and birds) than in ectotherms (Amphibia, Squamata, Testudines, and Crocodylia) (Hartman and Lessler 1964; Snyder and Sheafor 1999; Soslau 2020). It has been suggested that the acquisition of lungs together with the subsequent evolution of the cardiovascular system was the driving force explaining the evolution of vertebrate RBC_{size} (Snyder and Sheafor 1999). In endotherms, thermogenetic mechanisms use a huge amount of oxygen, producing high RMRs. Considering that “Smaller capillaries [and smaller RBCs] are associated with increased potential for diffusive gas exchange” (Snyder and Sheafor 1999: 189), these features may have been positively selected in endotherms. Huttenlocker and Farmer (2017) found that RBC_{size} values are related to, and can be inferred from, bone vascular canal diameter. Cubo et al. (2020) inferred notosuchian RBC_{size} values using this last relationship and concluded that they were significantly higher than the threshold separating ectotherms from endotherms.

To sum up, both proxies (RMR and RBC_{size}) suggest that Notosuchia were ectothermic organisms. Considering that paleohistological evidence (suggesting low RMR, large RBC_{size} , and ectothermy) is not congruent with morphological evidence (suggesting an erect posture, cursoriality, and endothermy), the

thermophysiological status (i.e., either ectothermic or endothermic) of Notosuchia deserves further analysis.

The approach used by Cubo et al. (2020) to perform these inferences can be improved in two ways. First, notosuchian thermophysiological status inferred using RBC_{size} is based on the quoted relationship between RBC_{size} and bone vascular canal diameter (Cubo et al. 2020). This relationship was tested by Huttenlocker and Farmer (2017) using a rather small sample size (14 extant tetrapod species). Here we tested this relationship using a more comprehensive sample of extant tetrapods (31 species) and phylogenetic generalized least-squares regression (PGLS). Second, RBC_{size} estimations were performed using phylogenetic eigenvector maps (PEMs), and this method excludes a fraction of phylogenetic information. This is because PEM generates a high number of eigenvectors ($n - 1$, with n being the number of terminal taxa analyzed), thus requiring a selection procedure to compile a subset of eigenvectors to avoid model overfitting (Guénard et al. 2013; Legendre et al. 2016). Here we inferred the thermophysiology of Notosuchia using phylogenetic logistic regression (PLR) (Ives and Garland 2010; Tung Ho and Ané 2014), a method that overcomes this problem, because it includes all (instead of a fraction) of the phylogenetic information.

Material and Methods

Phylogenies in Figure 1 and Supplementary File 1 contain the tetrapod samples used in this study. Topologies were taken from Pyron and Wiens (2011) for amphibians; Meredith et al. (2011), Zurano et al. (2019), Kumar et al. (2013), and Upham et al. (2019) for mammals; Ast (2001) and Villa et al. (2018) for *Varanus*; Man et al. (2011) for crocodiles; Prum et al. (2015) for birds; and Pol et al. (2014) for Notosuchia. Both phylogenies were dated using Time Tree of Life (<http://www.timetree.org>). When the ages of two successive nodes collapsed, we arbitrarily added 1 Myr in between the more-inclusive and less-inclusive nodes to facilitate the graphic visualization of the topology. For Notosuchia, nodes were dated according to the last appearance datum (LAD) of the oldest

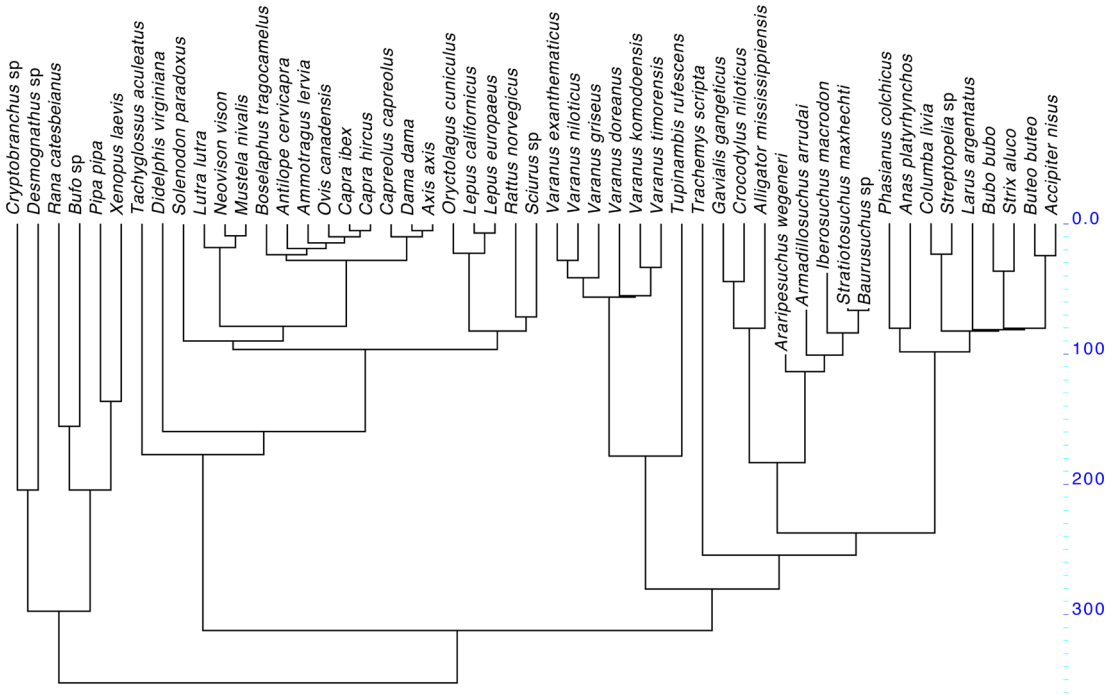


FIGURE 1. Phylogenetic relationships among extant taxa used to construct the thermophysiology inference model and the extinct Notosuchia for which we performed paleobiological inferences. Sources of topology and divergence times are cited in the main text. Scale on the right: geologic time in millions of years (Myr).

fossil included in each node taken from the Paleobiology Database (<https://paleobiodb.org>). The age of the node Notosuchia (113 Myr) corresponds to the LAD of *Malawisuchus mwakasyungutiensis*. The age of the node *Armadillosuchus–Baurusuchus* (100.5 Myr) corresponds to the LAD of *Chimaerasuchus paradoxus*. The age of the node *Iberosuchus–Baurusuchus* (83.6 Myr) corresponds to the LAD of *Comahuesuchus brachybuccalis*, *Pehuenchesuchus enderi*, *Cynodontosuchus rothi*, and *Wargosuchus australis*. Finally, the age of the node *Stratiotosuchus–Baurusuchus* (66 Myr) corresponds to the LAD of these taxa. The latter (*Stratiotosuchus–Baurusuchus*), as well as *Armadillosuchus arrudai*, come from the Adamantina Formation, the age of which is still debated. We follow the hypothesis of a Campanian–Maastrichtian age proposed by some authors (e.g., Gobbo-Rodrigues et al. 1999; Batezelli 2017).

Testing the Relationship between RBC_{size} and Bone Vascular Canal Diameter Using PGLS.—Supplementary File 1 contains the sample (31 species of extant tetrapods) and the

phylogeny (topology and divergence times) used to test the relationships between the response variables (RBC_{width} and RBC_{area}) and the explanatory variables (femoral vascular canal diameter and femoral cross-sectional area including the medullary cavity). Thin sections of extant taxa are curated at the Vertebrate Hard Tissue Collection of the Museum national d’Histoire naturelle, Paris, and are available on request to the curator (D. Germain). RBC_{width} (defined as RBC minimum diameter) and RBC_{area} (either published values or values computed using maximum and minimum published diameters and assuming an ellipse) were taken from the literature (Supplementary File 2). Femoral vascular canal diameters (white arrowheads in Fig. 2) were computed as Can_{harmean} and Can_{minv} as defined by Huttenlocker and Farmer (2017). Can_{harmean}, Can_{minv} and femoral cross-sectional area were either quantified in this study or taken from Huttenlocker and Farmer (2017) (data available in Supplementary File 2).

The method of ordinary least-squares regression makes the assumption of no covariance

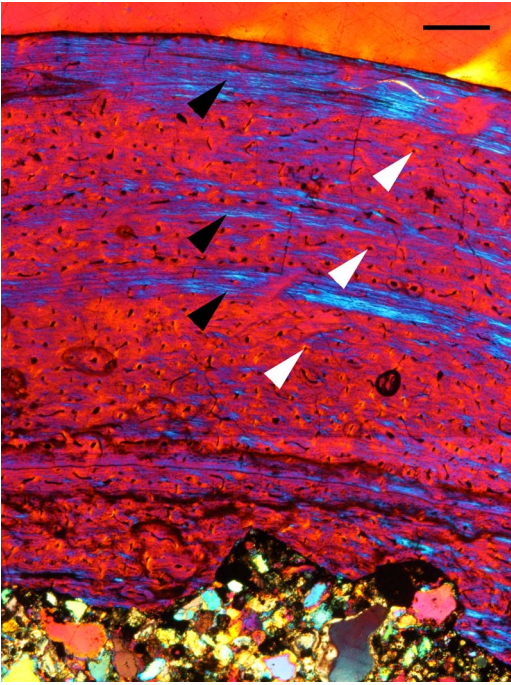


FIGURE 2. Transverse thin section, lateral side, of the femur of *Araripesuchus wegneri* Buffetaut, 1981, observed in cross-polarized light with lambda wave plate. The thin section was made from a partial femur (MNHN.F.GDF660) from the Aptian of Gadoufaoua (Niger), and is curated at the Museum national d’Histoire naturelle (MNHN) (Paris, France). The cortex is made of lamellar-zonal bone. It is composed of three zones formed at moderate growth rate and containing vascular canals (white arrowheads) included in primary osteons, and three annuli formed at low growth rates and made of parallel fibrous bone (black arrowheads). Periosteum is on the top and medullary cavity on the bottom. The continuous black line occurring near the medullary cavity is an artifact. Scale bar, 0.5 mm.

between residuals obtained from the regression equation (i.e., the off-diagonals of the variance–covariance matrix are expected to contain zeros) (Symonds and Blomberg 2014). In analyses using interspecific data, this assumption is not verified because of the hierarchical, shared phylogenetic history among terminal taxa (i.e., closely related species are more similar than expected by chance). PGLS (Grafen 1989; Martins and Hansen 1996; Rohlf 2001; Symonds and Blomberg 2014) overcomes this problem by using a variance–covariance matrix in which off-diagonals correspond to the phylogenetic history shared by the two species under comparison. Symonds and Blomberg (2014) described PGLS as a “weighted regression” in which data points corresponding to

closely related species are “downweighted.” We ran PGLS using the function *pgls* of the package *caper* (Orme et al. 2013) in R (R Development Core Team 2008).

Inferring the Thermophysiology of Notosuchia Using PLR.—Figure 1 shows the phylogenetic relationships among extant taxa (46 species of tetrapods) used to construct the thermophysiology inference model (to infer the probability of being endothermic) and the extinct Notosuchia for which we performed paleobiological inferences. This model was constructed using femoral vascular canal diameter (Can_{harmean} and Can_{min}) and femoral cross-sectional area as explanatory variables. As noted earlier, femoral Can_{harmean} , Can_{min} , and femoral cross-sectional area were either quantified in this study or taken from Huttenlocker and Farmer (2017) (data available in Supplementary File 3). As before, thin sections of extant taxa are curated at the Vertebrate Hard Tissue Collection of the Museum national d’Histoire naturelle, Paris. Data for Notosuchia are taken from Cubo et al. (2020): *Araripesuchus wegneri*, *Armadillosuchus arrudai*, *Baurusuchus* sp., *Iberosuchus macrodon*, and *Stratiotosuchus maxhechti*. Considering that the model was constructed using femora of extant species, we performed inferences only for those Notosuchia for which data for femora were available. Sample size was smaller for PGLS analyses, because data for RBC_{size} were not available for many species analyzed in PLR analyses. PLR is a generalized linear model explaining the probability of occurrence of the state “presence” of a binary response (dependent) variable (here the “presence of endothermy”) using continuous explanatory (independent) variables when residual variation of the former variable is phylogenetically structured (Ives and Garland 2010). The regression coefficients computed do account for phylogenetic correlation; when data are not phylogenetically structured, these coefficients are those of standard logistic regression (Ives and Garland 2010). PLR models contain two components. The first is controlled by parameters α (the transition rate) and μ (the asymptotic probability of being in state 1 [here the asymptotic probability of being endotherm]). Parameter α equals $\alpha_1 + \alpha_0$; α_1 being the probability that the response

variable switches from 0 to 1 in each small time increment when it evolves up a phylogenetic tree, whereas the α_0 parameter is the probability that it evolves from 1 to 0 (Ives and Garland 2010). The transition rate α is a measure of phylogenetic signal, because the larger the α , the quicker the evolutionary transitions and the lower the phylogenetic structure of data (Ives and Garland 2010). In the second component, the probability of occurrence of the state “presence of endothermy” is modeled using values of the independent (explanatory) variable (here bone vascular canal diameter). Parameters α and μ are estimated using an iterative process in which μ is estimated given α , using the quasi-likelihood function, and α is estimated given μ , using least squares until convergence (Ives and Garland 2010). Analyses were performed using the package *phyloglm* (Tung Ho and Ané 2014) in R (R Development Core Team 2008).

Results

Testing the Relationship between RBC_{size} and Bone Vascular Canal Diameter Using PGLS.—We used PGLS to test the relationships between RBC_{width} and RBC_{area} and the explanatory variables femoral vascular canal diameter (computed as Can_{harmean} and Can_{min}) and femoral cross-sectional area (data available in Supplementary File 2). Shapiro-Wilk normality tests showed that residuals of PGLS regression of RBC_{area} to Can_{harmean} + bone cross-sectional area and the regression RBC_{area} to Can_{min} + bone cross-sectional area do not follow a normal distribution (*p*-values of 0.0007557 and 0.001896, respectively). Thus, we performed a log transformation of all variables. After log transformation, residuals of all four PGLS regressions (RBC_{area} and RBC_{area} to the explanatory variables bone cross-sectional area and either Can_{min} or Can_{harmean}) do follow a normal distribution. All four of these PGLS regressions were significant and, in each regression, both explanatory variables (bone cross-sectional area and either Can_{min} or Can_{harmean}) were significant (Table 1).

Inferring the Thermophysiology of Notosuchia Using PLR.—We used PLR to construct models aimed at computing the probability of being

endothermic using paleohistological features (data available in Supplementary File 3). When Can_{harmean} was used as the explanatory variable, we obtained a model with a transition rate α of 0.00144, an intercept estimate of 6.04 (*p*-value = 0.004) and an estimate for the coefficient of Can_{harmean} of -0.45 (*p*-value = 0.001). The negative sign of the Can_{harmean} coefficient indicates that the probability of being endothermic decreases as vascular canal diameter increases. Figure 3 shows the distribution of probabilities of being endothermic as a function of Can_{harmean} variation. The corresponding equation is:

$$\ln[p(\text{endothermy})/p(\text{ectothermy})] = -0.45 * \text{Can}_{\text{harmean}} + 6.04 \quad (1)$$

or

$$p(\text{endothermy}) = \frac{\exp(-0.45 * \text{Can}_{\text{harmean}} + 6.04)}{[1 + \exp(-0.45 * \text{Can}_{\text{harmean}} + 6.04)]} \quad (2)$$

Ives and Garland (2010: p. 17) stated that “we assume that if $\mu_i < \bar{\mu}$, then trait Y will evolve toward 0; [...] Conversely, if $\mu_i > \bar{\mu}$, then trait Y will evolve toward 1,” where $\bar{\mu}$ is the mean probability of being endotherm in our sample. Thus, we considered that $\bar{\mu}$ is the cutoff probability, so that an inferred probability higher than $\bar{\mu}$ would be evidence for endothermy. Conversely, a probability lower than $\bar{\mu}$ would be evidence for ectothermy. When Can_{harmean} was used as the explanatory variable, $\bar{\mu} = 0.59$. To evaluate the predictive power of the model, we constructed a contingency table in which we inferred the thermometabolic regime of each extant species of the sample using its Can_{harmean}. Lines contain predictions (0, inferred ectothermy; 1, inferred endothermy) and columns contain true states (0, observed ectothermy; 1, observed endothermy):

	state 0	state 1
prediction 0	14	2
prediction 1	3	27

The specificity (the ratio of quantity of true 1 inferred as 1 on the quantity of true 1; $Sp = 27 / (27 + 2)$) equals 0.931. The sensitivity (the ratio of quantity of true 0 inferred as 0 on the quantity of true 0; $Se = 14 / (14 + 3)$) equals 0.824. The

TABLE 1. Testing the relationship between the dependent variables used to quantify red blood cell size (RBC_{size} , RBC_{width} and RBC_{area}) and the explanatory variables femoral vascular canal diameter (computed either as Can_{min} or $Can_{harmean}$) and femoral cross-sectional area using phylogenetic generalized least-squares regression. * p -value < 0.05; ** p -value < 0.01; *** p -value < 0.001.

Dependent (response) variable	Adjusted R^2		Estimate	p -value
RBC_{width}	0.624	Intercept	0.895	0.001603**
		Can_{min}	0.714	2.08×10^{-6} ***
		Bone cross-sectional area	-0.095	0.001249**
RBC_{width}	0.341	Intercept	1.250	0.000888***
		$Can_{harmean}$	0.459	0.001557**
		Bone cross-sectional area	-0.101	0.006239**
RBC_{area}	0.399	Intercept	1.910	0.016427*
		Can_{min}	1.398	0.000315***
		Bone cross-sectional area	-0.158	0.027307*
RBC_{area}	0.189	Intercept	2.757	0.002499**
		$Can_{harmean}$	0.852	0.013002*
		Bone cross-sectional area	-0.176	0.043913*

classification error (the ratio (quantity of true 0 inferred as 1 + quantity of true 1 inferred as 0)/ total; error = $(3 + 2)/(14 + 2 + 3 + 27)$) equals 0.109. This classification error is quite low, so we used the cutoff probability of 0.59 to perform paleobiological inferences using $Can_{harmean}$ as the explanatory (predictor) variable.

When Can_{min} was used as the explanatory variable, we obtained a model with a transition rate α of 0.00052, an intercept estimate of 2.58 (p -value = 0.032), and an estimate for the

coefficient of Can_{min} of -0.49 (p -value = 0.018). Figure 4 shows the distribution of probabilities of being endothermic as a function of Can_{min} variation. The corresponding equation is:

$$\ln[p(\text{endothermy})/p(\text{ectothermy})] = -0.49 * Can_{min} + 2.58 \tag{3}$$

or

$$p(\text{endothermy}) = \frac{\exp(-0.49 * Can_{min} + 2.58)}{[1 + \exp(-0.49 * Can_{min} + 2.58)]} \tag{4}$$

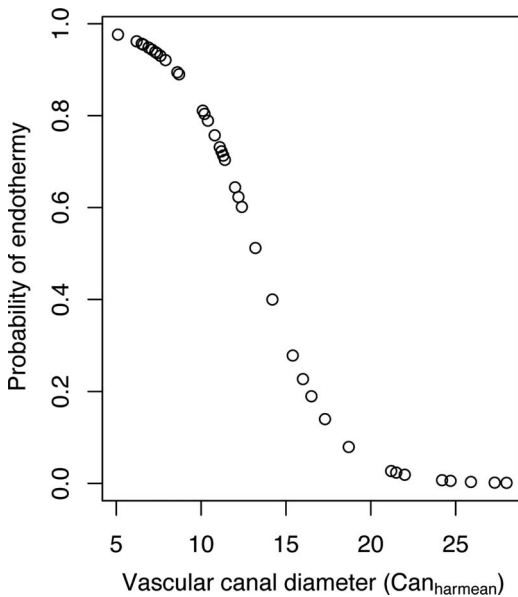


FIGURE 3. Distribution of probabilities of being endothermic inferred for our sample of extant tetrapods using a phylogenetic logistic regression model that includes femoral vascular canal diameter (computed as $Can_{harmean}$) as the explanatory variable.

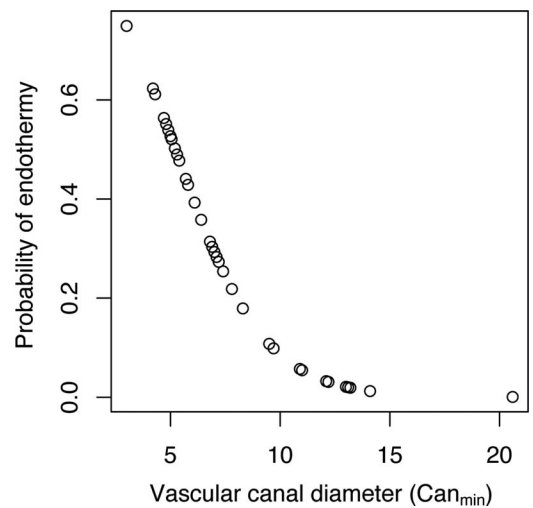


FIGURE 4. Distribution of probabilities of being endothermic inferred for our sample of extant tetrapods using a phylogenetic logistic regression model that includes femoral vascular canal diameter (computed as Can_{min}) as the explanatory variable.

Again we evaluated the quality of the model by constructing a contingency table in which we inferred the thermophysiological regime of each extant species of the sample using its Can_{min} . We used a cutoff probability of $\bar{\mu} = 0.32$ (the mean probability of being endothermic in our sample), so that an inferred probability lower than 0.32 is evidence for ectothermy and a probability higher than 0.32 is evidence for endothermy:

	state 0	state 1
prediction 0	15	9
prediction 1	2	20

The specificity (the ratio of quantity of true 1 inferred as 1 on the quantity of true 1; $Sp = 20/(20 + 9)$) equals 0.690. The sensitivity (the ratio of quantity of true 0 inferred as 0 on the quantity of true 0; $Se = 15/(15 + 2)$) equals 0.882. The classification error (the ratio (quantity of true 0 inferred as 1 + quantity of true 1 inferred as 0)/total; $error = (2 + 9)/(15 + 9 + 2 + 20)$) equals 0.239. This classification error is quite high, so we recomputed a new cutoff probability of 0.22 using the receiver operating characteristic curve. Then we constructed a new contingency table in which we inferred the thermophysiological regime of each extant species of the sample using its Can_{min} and considering that an inferred probability higher than 0.22 is evidence for endothermy:

	state 0	state 1
prediction 0	15	1
prediction 1	2	28

With this contingency table, the classification error [the ratio (quantity of true 0 inferred as 1 + quantity of true 1 inferred as 0)/total; $error = (2 + 1)/(15 + 1 + 2 + 28)$] equals 0.0652. This classification error is quite low, so we used the cutoff probability of 0.22 to perform paleobiological inferences using Can_{min} as the explanatory (predictor) variable.

We used these equations and cutoff probabilities and femoral $Can_{harmean}$ and Can_{min} values published by Cubo et al. (2020) for Notosuchia to compute the probability of these taxa being endotherms (Table 2).

Discussion

Notosuchia is an extremely diversified group of crocodyliforms. This diversity is particularly striking regarding their diet, suggesting that they occupied various ecological niches (Carvalho and Bertini 1999; Iori and Carvalho 2018). Uruguaysuchidae (Pol et al. 2014), the most basal notosuchians, of which *Araripesuchus wegeneri* (in our sample) is a representative, range from the Aptian (*Araripesuchus gomesii*) to the Maastrichtian (*Araripesuchus tsangatsangana*) (Price 1959; Turner 2006). Several species of this group have been inferred as being omnivorous, or even insectivorous, based on their dental complexity (Sereno and Larsson 2009; Soto et al. 2011; Nieto et al. 2021) and postcranial remains suggest that they had an erect posture (see “Introduction”). Uruguaysuchids were smaller than Sphagesauridae (Carvalho et al. 2010; Godoy et al. 2019). *Armadillosuchus* (also sampled by us) belongs to the large-bodied sphagesaurids group (Melstrom and Irmis 2019). The diagnosis of this clade is based on its peculiar dentition morphology (Price 1950). They show extremely complex manducatory systems, with evidence of “chewing” mechanisms, dental wear, and propalinal movements (e.g., see Ósi 2014; Iori and Carvalho 2018). The foraging abilities of some notosuchians, such as *Armadillosuchus*, *Mariliasuchus*, or *Mala-wisuchus*, to locate food or water have led some authors to propose the presence of burrowing habits (Gomani 1997; Nobre et al. 2008; Marinho and Carvalho 2009), a behavior that might play a role in thermoregulation (e.g., to search for a cooler shelter during dry periods, as in extant crocodylian species; Campos and Magnusson 2013). This behavior has also been proposed for the sebecosuchian *Baurusuchus salgadoensis* (Vasconcellos and Carvalho 2010). Sebecosuchia (to which *Iberosuchus* and *Stratiotosuchus*, also sampled by us, belong) were large predators with an erect posture (see “Introduction”) and cursorial abilities (Nascimento and Zaher 2010; Riff and Kellner 2011), feeding on large prey, including small sphagesaurids (Godoy et al. 2014). Indeed, their ziphodont teeth (unicuspidated, laterally compressed with serrated carinae) associated with the biomechanical performances of their skull allowed sebecosuchians

TABLE 2. Inferring the probability of endothermy for the sample of *Notosuchia* analyzed in this study using femoral vascular canal diameters (computed either as Can_{min} or $Can_{harmean}$) as explanatory variables and phylogenetic logistic regressions. Vascular canal diameters for *Notosuchia* were taken from Cubo et al. (2020).

	$Can_{harmean}$	Probability of being endothermic	Inferred status at cutoff probability of 0.59	Can_{min}	Probability of being endothermic	Inferred status at cutoff probability of 0.22
<i>Araripesuchus wegeneri</i>	25.99	0.0035	Ectothermy	13	0.0221	Ectothermy
<i>Armadillosuchus arrudai</i>	25.32	0.0047	Ectothermy	13.36	0.0186	Ectothermy
<i>Baurusuchus</i> sp.	25.02	0.0054	Ectothermy	12.67	0.0259	Ectothermy
<i>Iberosuchus macrodon</i>	31.76	0.0003	Ectothermy	14	0.0137	Ectothermy
<i>Stratiotosuchus maxhechti</i>	31.55	0.0003	Ectothermy	14.87	0.0090	Ectothermy

to effectively handle prey after wounding it (Montefeltro et al. 2020). It is noteworthy that the inferred ectothermic sebecosuchians occupy a niche usually occupied by endothermic theropod dinosaurs (Benson et al. 2013; Zanno and Makovicky 2013).

The ectothermic condition of *Notosuchia* suggested by Cubo et al. (2020) is supported by the results of the present study using larger sample sizes of extant species and a more robust phylogenetic comparative method (PLR). First, the finding that RBC_{size} is related to bone vascular canal diameter (Huttenlocker and Farmer 2017) is supported by our results obtained using a sample size more than twice of that used by these authors. Thus bone vascular canal diameter can be used as a proxy to infer RBC_{size} , and then endothermy (because within tetrapods, RBC_{size} is lower in endotherms than in ectotherms; Snyder and Sheafor 1999). Huttenlocker and Farmer (2017) included bone cross-sectional area (in addition to bone vascular canal diameter) as an explanatory variable in models aimed at explaining the variation of RBC_{size} . However, in their study, bone cross-sectional area did not improve the explanatory power of models and was not retained (Huttenlocker and Farmer 2017; Supplemental Information, “Analysis I, Training Data Set for Extant Taxa”). Unexpectedly, our analyses (using a larger sample size) showed that bone cross-sectional area significantly improves the explanatory power of models and is retained, together with bone vascular canal diameter, in models explaining the variation of RBC_{size} . The fact

that the estimate for bone cross-sectional area is always negative (Table 1) indicates that RBC_{size} decreases as bone cross-sectional area increases. Second, notosuchian thermometabolism is inferred here using a larger sample of extant tetrapods (more than three times the sample used by Cubo et al. [2020]) and logistic phylogenetic regressions (a method more reliable than those used in previous studies; see below). We are aware of the fact that Huttenlocker and Farmer (2017) showed that histological changes reflect changes in VO_{2max} better than changes in thermometabolism. However, we have found here that microstructural variation is linked to thermometabolism too. The models constructed to infer the probability of endothermy using vascular canal size as an explanatory (predictive) variable were highly significant, and the classification errors obtained are quite low (6.5% using Can_{min}). Thus we conclude that we can use these models confidently in paleobiological inference of thermometabolism.

Thermal paleophysiology is an emergent discipline (Cubo and Huttenlocker 2020). It has great potential resulting from the synergy between physiological studies aimed at deciphering the mechanisms of thermogenesis in extant amniotes (e.g., Bal and Periasamy 2020; Jastroch and Seebacher 2020; Grigg et al. 2021) and paleobiological inferences in extinct amniotes using phylogenetic comparative methods (e.g., Cubo et al. 2012, 2020, 2022; Legendre et al. 2016; Huttenlocker and Farmer 2017; Olivier et al. 2017; Fleischle et al. 2018; Cubo and Jalil 2019; Faure-Brac et al. 2021;

Knaus et al. 2021). Logistic phylogenetic regressions are the third step in efforts performed during the last decade to carry out reliable inferences of thermometabolic status in extinct amniotes. A decade ago, Cubo et al. (2012) inferred bone growth rates using bone histological features and multiple linear regressions tested for significance using permutations in order to circumvent the nonindependence of the observations due to the phylogeny. Considering that bone growth rates are significantly related to RMR in amniotes (Montes et al. 2007), the former was used by Cubo et al. (2012) as a proxy to infer the thermometabolic status of extinct archosaurs. This method was used by Legendre et al. (2013) to infer the bone growth rate and the thermometabolic status of *Euparkeria*. In a second step, Legendre et al. (2016) adapted Guénard et al.'s (2013) PEMs to perform paleobiological inferences of RMR. This contribution represented significant methodological progress, because paleobiological inference models included the phylogeny (rather than circumventing its effects, as did the preceding method), assuming an evolutionary model (Molina-Venegas et al. 2018). PEMs have been widely used to infer the thermometabolic status of extinct amniotes (Legendre et al. 2016; Olivier et al. 2017; Fleischle et al. 2018; Cubo and Jalil 2019; Cubo et al. 2020, 2022; Faure-Brac and Cubo 2020; Faure-Brac et al. 2021; Knaus et al. 2021). Using logistic phylogenetic regressions is a new step in this sequence. This method improves upon the previous approach by using all of the phylogenetic information (rather than a fraction of it, as did PEMs in order to avoid model overfitting). An encouraging sign is that results are congruent in spite of the diversity of methods used to obtain them. Inferring the maximum metabolic rate of *Notosuchia* using the size of femoral nutrient foramina (Seymour et al. 2012) would be the next promising step to fully understand the thermophysiology of these amazing crocodylomorphs.

Acknowledgments

We thank H. Lamrous (Sorbonne Université) for helping us with picture acquisition using bone thin sections at the Vertebrate Hard

Tissue Collection of the Museum national d'Histoire naturelle (Paris). This study was partly funded by the project Emergences Sorbonne Université 2019 no. 243374 to J.C. The authors declare no competing interests.

Data Availability Statement

Data available from the Dryad and Zenodo Digital Repositories: <https://doi.org/10.5061/dryad.80gb5mktb>, <https://doi.org/10.5281/zenodo.6795231>.

Literature Cited

- Andrews, R. M., and F. H. Pough. 1985. Metabolism of squamate reptiles: allometric and ecological relationships. *Physiological Zoology* 58:214–231.
- Ast, J. C. 2001. Mitochondrial DNA evidence and evolution in Varanoidea (Squamata). *Cladistics* 17:211–226.
- Bal, N. C., and M. Periasamy. 2020. Uncoupling of sarcoendoplasmic reticulum calcium ATPase pump activity by sarcolipin as the basis for muscle non-shivering thermogenesis. *Philosophical Transactions of the Royal Society of London B* 375:20190135.
- Batezelli, A. 2017. Continental systems tracts of the Brazilian Cretaceous Bauru Basin and their relationship with the tectonic and climatic evolution of South America. *Basin Research* 29:1–25.
- Benson, R. B. J., P. D. Mannion, R. J. Butler, P. Upchurch, A. Goswami, and S. E. Evans. 2013. Cretaceous tetrapod fossil record sampling and faunal turnover: implications for biogeography and the rise of modern clades. *Palaeogeography, Palaeoclimatology, Palaeoecology* 372:88–107.
- Buffetaut, E. 1981. Die biogeographische Geschichte der Krokodilier, mit Beschreibung einer neuen Art, *Araripesuchus wegneri*. *Geologische Rundschau* 70:611–624.
- Campos, Z., and W. E. Magnusson. 2013. Thermal relations of dwarf caiman, *Paleosuchus palpebrosus*, in a hillside stream: evidence for an unusual thermal niche among crocodylians. *Journal of Thermal Biology* 38:20–23.
- Carrier, D. R. 1987. The evolution of locomotor stamina in tetrapods: circumventing a mechanical constraint. *Paleobiology* 13:326–341.
- Carvalho, I. S., and R. J. Bertini. 1999. *Mariliaesuchus*: um novo Crocodylomorpha (Notosuchia) do Cretáceo da Bacia Bauru. *Geologia Colombiana* 24:83–105.
- Carvalho, I. de S., Z. B. de Gasparini, L. Salgado, F. M. de Vasconcelos, and T. da S. Marinho. 2010. Climate's role in the distribution of the Cretaceous terrestrial Crocodyliformes throughout Gondwana. *Palaeogeography, Palaeoclimatology, Palaeoecology* 297:252–262.
- Clarke, A., and H.-O. Pörtner. 2010. Temperature, metabolic power and the evolution of endothermy. *Biological Reviews* 85:703–727.
- Cubo, J., and A. K. Huttenlocker. 2020. Vertebrate palaeophysiology. *Philosophical Transactions of the Royal Society of London B* 375:20190130.
- Cubo, J., and N.-E. Jalil. 2019. Bone histology of *Azendohsaurus laaroussii*: implications for the evolution of thermometabolism in Archosauromorpha. *Paleobiology* 45:317–330.
- Cubo, J., N. Le Roy, C. Martínez-Maza, and L. Montes. 2012. Paleohistological estimation of bone growth rate in extinct archosaurs. *Paleobiology* 38:335–349.
- Cubo, J., M. V. A. Sena, P. Aubier, G. Houee, P. Claisse, M. G. Faure-Brac, R. Allain, R. C. L. P. Andrade, J. M. Sayão, and G. R. Oliveira. 2020. Were Notosuchia (Pseudosuchia:

- Crocodylomorpha) warm-blooded? A palaeohistological analysis suggests ectothermy. *Biological Journal of the Linnean Society* 131:154–162.
- Cubo, J., A. D. Buscalioni, L. J. Legendre, E. Bourdon, J. L. Sanz and A. de Ricqlès. 2022. Palaeohistological inferences of resting metabolic rates in *Concornis* and *Iberomesornis* (Enantiornithes, Ornithothoraces) from the Lower Cretaceous of Las Hoyas (Spain). *Palaeontology* 65:e12583.
- Faure-Brac, M. G., and J. Cubo. 2020. Were the synapsids primitively endotherms? A palaeohistological approach using phylogenetic eigenvector maps. *Philosophical Transactions of the Royal Society of London B* 375:20190138.
- Faure-Brac, M. G., R. Amiot, C. de Muizon, J. Cubo, and C. Lécuyer. 2021. Combined paleohistological and isotopic inferences of thermometabolism in extinct Neosuchia, using *Goniopholis* and *Dyrosaurus* (Pseudosuchia: Crocodylomorpha) as case studies. *Paleobiology* 48:302–323.
- Fleischle, C. V., T. Wintrich, and P. M. Sander. 2018. Quantitative histological models suggest endothermy in plesiosaurs. *PeerJ* 6:e4955.
- Gobbo-Rodrigues S. R., S. Petri and R. J. Bertini. 1999. Ocorrências de ostrácodos na Formação Araçatuba do Grupo Bauru, Cretáceo Superior da Bacia do Paraná e possibilidades de correlação com depósitos isócronos argentinos—parte i: Família Hylocypridae. *Acta Geologica Leopoldensia* 23:3–13.
- Godoy, P. L., F. C. Montefeltro, M. A. Norell, and M. C. Langer. 2014. An additional Baurusuchid from the Cretaceous of Brazil with evidence of interspecific predation among Crocodyliformes. *PLoS ONE* 9:e97138.
- Godoy, P. L., M. Bronzati, E. Eltink, J. C. A. Marsola, G. M. Cidade, M. Langer, and F. Montefeltro. 2016. Postcranial anatomy of *Pisarrachampsya sera* (Crocodyliformes, Baurusuchidae) from the Late Cretaceous of Brazil: insights on lifestyle and phylogenetic significance. *PeerJ* 4:e2075.
- Godoy, P. L., R. B. J. Benson, M. Bronzati, and R. J. Butler. 2019. The multi-peak adaptive landscape of crocodylomorph body size evolution. *BMC Evolutionary Biology* 19:167.
- Gomani, E. M. 1997. A crocodyliform from the Early Cretaceous Dinosaur Beds, northern Malawi. *Journal of Vertebrate Paleontology* 17:280–294.
- Grafen, A. 1989. The phylogenetic regression. *Philosophical Transactions of the Royal Society of London B* 326:119–157.
- Grigg, G., J. Nowack, J. E. Bicudo, W. Pereira, N. C. Bal, H. N. Woodward, and R. S. Seymour. 2021. Whole-body endothermy: ancient, homologous and widespread among the ancestors of mammals, birds and crocodylians. *Biological Reviews* 97:766–801.
- Guénard, G., P. Legendre, and P. Peres-Neto. 2013. Phylogenetic eigenvector maps: a framework to model and predict species traits. *Methods in Ecology and Evolution* 4:1120–1131.
- Hartman, F. A., and M. A. Lessler. 1964. Erythrocyte measurements in fishes, amphibia and reptiles. *Biological Bulletin* 126:83–88.
- Huttenlocker, A. K., and C. G. Farmer. 2017. Bone microvasculature tracks red blood cell size diminution in Triassic mammal and dinosaur forelimbs. *Current Biology* 27:48–54.
- Iori, F.V., and I. S. Carvalho. 2018. The Cretaceous crocodyliform *Caipirasuchus*: behavioral feeding mechanisms. *Cretaceous Research* 84:181–187.
- Ives, A. R., and T. Garland. 2010. Phylogenetic logistic regression for binary dependent variables. *Systematic Biology* 59:9–26.
- Jastroch, M., and F. Seebacher. 2020. Importance of adipocyte browning in the evolution of endothermy. *Philosophical Transactions of the Royal Society of London B* 375:20190134.
- Knaus, P. L., A. H. Van Heteren, J. K. Lungmus, and P. M. Sander. 2021. High blood flow into the femur indicates elevated aerobic capacity in synapsids since the reptile-mammal split. *Frontiers in Ecology and Evolution* 9:751238.
- Kumar, V., B. M. Hallström, and A. Janke. 2013. Coalescent-based genome analyses resolve the early branches of the Euarchontoglires. *PLoS ONE* 8:e60019.
- Legendre, L. J., and D. Davesne. 2020. The evolution of mechanisms involved in vertebrate endothermy. *Philosophical Transactions of the Royal Society of London B* 375:20190136.
- Legendre, L. J., L. Segalen, and J. Cubo. 2013. Evidence for high bone growth rate in *Euparkeria* obtained using a new paleohistological inference model for the humerus. *Journal of Vertebrate Paleontology* 33:1343–1350.
- Legendre, L. J., G. Guénard, J. Botha-Brink, and J. Cubo. 2016. Palaeohistological evidence for ancestral high metabolic rate in archosaurs. *Systematic Biology* 65:989–996.
- Man, Z., W. Yishu, Y. Peng, and W. Xiaobing. 2011. Crocodylian phylogeny inferred from twelve mitochondrial protein-coding genes, with new complete mitochondrial genomic sequences for *Crocodylus acutus* and *Crocodylus novaeguinae*. *Molecular Phylogenetics and Evolution* 60:62–67.
- Marinho, T. S., and I. S. Carvalho. 2009. An armadillo-like sphageosaurid crocodyliform from the Late Cretaceous of Brazil. *Journal of South American Earth Sciences* 27:36–41.
- Martins, E. P., and T. F. Hansen. 1996. The statistical analysis of interspecific data: a review and evaluation of phylogenetic comparative methods. Pp. 22–75 in E. P. Martins, ed. *Phylogenies and the comparative method in animal behavior*. Oxford University Press, New York.
- Melstrom, K. M., and R. B. Iris. 2019. Repeated evolution of herbivorous crocodyliforms during the age of dinosaurs. *Current Biology* 29:2389–2395.e3.
- Meredith, R. W., J. E. Janečka, J. Gatesy, O. A. Ryder, C. A. Fisher, E. C. Teeling, A. Goodbla, E. Eizirik, T. L. L. Simão, T. Stadler, D. L. Rabosky, R. L. Honeycutt, J. J. Flynn, C. M. Ingram, C. Steiner, T. L. Williams, T. J. Robinson, A. Burk-Herrick, M. Westerman, N. A. Ayoub, M. S. Springer, and W. J. Murphy. 2011. Impacts of the cretaceous terrestrial revolution and KPg extinction on mammal diversification. *Science* 334:521–524.
- Molina-Venegas, R., J. C. Moreno-Saiz, I. Castro Parga, T. J. Davies, P. R. Peres-Neto, and M. Á. Rodríguez. 2018. Assessing among-lineage variability in phylogenetic imputation of functional trait datasets. *Ecography* 41:1740–1749.
- Montefeltro, F. C., S. Lautenschlager, P. L. Godoy, G. S. Ferreira, and R. J. Butler. 2020. A unique predator in a unique ecosystem: modelling the apex predator within a Late Cretaceous crocodyliform-dominated fauna from Brazil. *Journal of Anatomy* 237:323–333.
- Montes, L., N. Le Roy, M. Perret, V. de Buffrénil, J. Castanet, and J. Cubo. 2007. Relationships between bone growth rate, body mass and resting metabolic rate in growing amniotes: a phylogenetic approach. *Biological Journal of the Linnean Society* 92:63–76.
- Nascimento, P. M., and H. Zaher. 2010. A new species of *Baurusuchus* (Crocodyliformes, Mesoeucrocodylia) from the Upper Cretaceous of Brazil, with the first complete postcranial skeleton described for the family Baurusuchidae. *Papéis Avulsos de Zoologia* 50:323–361.
- Nieto, M. N., F. J. Degrange, K. C. Sellers, D. Pol, and C. M. Holliday. 2021. Biomechanical performance of the cranio-mandibular complex of the small notosuchian *Arairipesuchus gomesii* (Notosuchia, Uruguaysuchidae). *Anatomical Record*, <https://doi.org/10.1002/ar.24697>.
- Nobre, P. H., I. de Souza Carvalho, F. M. de Vasconcelos, and P. R. Souto. 2008. Feeding behavior of the Gondwanic Crocodylomorpha *Mariliaesuchus amarali* from the Upper Cretaceous Bauru Basin, Brazil. *Gondwana Research* 13:139–145.
- Olivier, C., A. Houssaye, N.-E. Jalil, and J. Cubo. 2017. First palaeohistological inference of resting metabolic rate in an extinct synapsid, *Moghreberia nmachouensis* (Therapsida: Anomodontia). *Biological Journal of the Linnean Society* 121:409–419.
- Orme, D., R. Freckleton, G. H. Thomas, T. Petzoldt, S. Fritz, N. Isaac, and W. Pearse. 2013. Caper: comparative analyses of

- phylogenetics and evolution in R. <https://CRAN.R-project.org/package=caper>, accessed 23 May 2022.
- Ósi, A. 2014. The evolution of jaw mechanism and dental function in heterodont crocodyliforms. *Historical Biology* 26:279–414.
- Pol, D. 2005. Postcranial remains of *Notosuchus terrestris* Woodward (Archosauria: Crocodyliformes) from the upper Cretaceous of Patagonia, Argentina. *Ameghiniana* 42:21–38.
- Pol, D., P. M. Nascimento, A. B. Carvalho, C. Riccomini, R. A. Pires-Domingues, and H. Zaher. 2014. A new notosuchian from the Late Cretaceous of Brazil and the phylogeny of advanced notosuchians. *PLoS ONE* 9:e93105.
- Price, L. I. 1950. On a new Crocodylia, *Sphagesaurus* from the Cretaceous of State of São Paulo, Brazil. *Anais da Academia Brasileira de Ciências* 22:77–83.
- Price, L. I. 1959. Sobre um crocodilídeo notossuquío do Cretácico Brasileiro. Serviço Gráfico do Instituto Brasileiro de Geografia e Estatística, Rio de Janeiro.
- Prum, R. O., J. S. Berv, A. Dornburg, D. J. Field, J. P. Townsend, E. M. Lemmon, and A. R. Lemmon. 2015. A comprehensive phylogeny of birds (Aves) using targeted next-generation DNA sequencing. *Nature* 526:569–573.
- Pyron, R. A., and J. J. Wiens. 2011. A large-scale phylogeny of Amphibia including over 2800 species, and a revised classification of extant frogs, salamanders, and caecilians. *Molecular Phylogenetics and Evolution* 61:543–583.
- R Development Core Team. 2008. R: a language and environment for statistical computing. R Foundation for Statistical Computing, Vienna, Austria.
- Riff, D., and A. W. A. Kellner. 2011. Baurusuchid crocodyliforms as theropod mimics: clues from the skull and appendicular morphology of *Stratiotosuchus maxhechti* (Upper Cretaceous of Brazil). *Zoological Journal of the Linnean Society* 163:S37–S56.
- Rohlf, F. J. 2001. Comparative methods for the analysis of continuous variables: geometric interpretations. *Evolution* 55:2143–2160.
- Sereno, P., and H. Larsson. 2009. Cretaceous crocodyliforms from the Sahara. *ZooKeys* 28:1–143.
- Seymour, R. S., S. L. Smith, C. R. White, D. M. Henderson, and D. Schwarz-Wings. 2012. Blood flow to long bones indicates activity metabolism in mammals, reptiles and dinosaurs. *Proceedings of the Royal Society of London B* 279:451–456.
- Snyder, G. K., and B. A. Sheafor. 1999. Red blood cells: centerpiece in the evolution of the vertebrate circulatory system. *Integrative and Comparative Biology* 39:189–198.
- Soslau, G. 2020. The role of the red blood cell and platelet in the evolution of mammalian and avian endothermy. *Journal of Experimental Zoology B* 334:113–127.
- Soto, M., D. Pol, and D. Perea. 2011. A new specimen of *Uruguaysuchus aznarezi* (Crocodyliformes: Notosuchia) from the middle Cretaceous of Uruguay and its phylogenetic relationships. *Zoological Journal of the Linnean Society* 163:S173–S198.
- Symonds, M. R. E., and S. P. Blomberg. 2014. A primer on phylogenetic generalised least squares. Pp. 105–130 in L. Z. Garamszegi, ed. *Modern phylogenetic comparative methods and their application in evolutionary biology: concepts and practice*. Springer, Berlin.
- Tung Ho, L.-s., and C. Ané. 2014. A linear-time algorithm for Gaussian and non-Gaussian trait evolution models. *Systematic Biology* 63:397–408.
- Turner, A. H. 2006. Osteology and phylogeny of a new species of *Araripesuchus* (Crocodyliformes: Mesoeucrocodylia) from the Late Cretaceous of Madagascar. *Historical Biology* 18:255–369.
- Upham, N. S., J. A. Esselstyn, and W. Jetz. 2019. Inferring the mammal tree: species-level sets of phylogenies for questions in ecology, evolution, and conservation. *PLoS Biology* 17:e3000494.
- Vasconcellos, F. M., and I. D. S. Carvalho. 2010. Paleontological assemblage associated with *Baurusuchus salgadoensis* remains, a Baurusuchidae Mesoeucrocodylia from the Bauru Basin, Brazil (Late Cretaceous). *Bulletin of the New Mexico Museum of Natural History and Science* 51:227–237.
- Villa, A., J. Abella, D. M. Alba, S. Almcija, A. Bolet, G. D. Koufos, F. Knoll, À. H. Luján, J. Morales, J. M. Robles, I. M. Sánchez, and M. Delfino. 2018. Revision of *Varanus marathonensis* (Squamata, Varanidae) based on historical and new material: morphology, systematics, and paleobiogeography of the European monitor lizards. *PLoS ONE* 13:e0207719.
- Wu, X.-C., and H.-D. Sues. 1996. Anatomy and phylogenetic relationships of *Chimaerasuchus paradoxus*, an unusual crocodyliform reptile from the Lower Cretaceous of Hubei, China. *Journal of Vertebrate Paleontology* 16:688–702.
- Zanno, L. E., and P. J. Makovicky. 2013. Neovenatorid theropods are apex predators in the Late Cretaceous of North America. *Nature Communications* 4:2827.
- Zurano, J. P., F. M. Magalhães, A. E. Asato, G. Silva, C. J. Bidau, D. O. Mesquita, and G. C. Costa. 2019. Cetartiodactyla: updating a time-calibrated molecular phylogeny. *Molecular Phylogenetics and Evolution* 133:256–262.